International Journal of Engineering & Technology, 7 (4.18) (2018) 311-315

International Journal of Engineering & Technology

Website: www.sciencepubco.com/index.php/IJET

Research paper

Nanocrystalline Cellulose Isolation from Pulverized Kenaf Core using Hydrothermal Treatment with Low Concentration of Oxalic Acid

Syaidatul Akma Mohd Zuki[1], Muhammad Shaifudin bin Azman[1], Norazah Abd Rahman[1*], Noor Fitrah Abu Bakar[1*]

[1]Faculty of Chemical Engineering, Universiti Teknologi MARA Shah Alam, 40450 Shah Alam, Selangor, Malaysia
**Corresponding author E-mail: noraz695@salam.uitm.edu.my, fitrah@salam.uitm.edu.my*

Abstract

Isolation of nanocrystalline celluloses (NCC) from pulverized kenaf core (PKC) particles using hydrothermal treatment with low concentration of oxalic acid hydrolysis was investigated in this study. Prior to hydrolysis treatment, PKC particles were pretreated using alkali (NaOH) and bleaching treatments to eliminate lignin and hemicellulose. Zeta potential and particles size analysis showed that the zeta potential value and the average size of NCC obtained is -31.6 mV and 182.55 nm respectively. The median diameter, d_{50} for the NCC suspension is 316.72 nm. A rough surface of flake shape agglomerated NCC particles was shown in SEM image. Fourier transform infrared (FTIR) spectroscopy showed the removal of lignin and hemicellulose after alkali treatment and bleaching process since there is no peak at wavelength number of 1740 and 1590 cm^{-1}. X-ray diffraction (XRD) analysis revealed that the crystallinity increased from 59.72% to 64.29%.

Keywords: *Pulverized kenaf core, Nanocrystalline cellulose, Hydrothermal, Oxalic Acid*

1. Introduction

Kenaf is natural fibres that have been studied extensively and receive attentions owing to their biodegradability, renewability and high quality equivalent to other synthetic fibres. In recent years, green, sustainable and environmental friendly materials have gain attentions for many applications. Therefore, the use of renewable and biodegradable biomass fibres reinforced composite materials has been established to get successive generation of ecological and green resources in this field. The productions of cellulosic fibres in nano dimensions known as nanocellulose enhance favourable properties for example high mechanical characteristics and low density besides its biodegradability and renewability.

'Nanocellulose' term generally denotes the cellulosic materials having any one dimension in the nanometer range. Nanocellulose can be synthesis from various lignocellulosic sources by different methods. Recently, cellulose nanofibres has caught significant interest due to their low thermal expansion, strengthening effect, high aspect ratio (length per diameter ratio), good mechanical and optical properties that may discover numerous applications in paper production, nanocomposites, coating additives, security papers and food packaging. Integration of ecological biomass nanoreinforcements such as cellulose nanofibres into other polymers has previously recognised to be the key approach for gaining nanocomposites with advanced mechanical performance [1]. Prodigious potentials for the progression of novel green nanocomposite resources are also offered by these biodegradable nanoreinforcements. Furthermore, it has also favourable application in many electrical devices.

Presently, the synthesis, characterization, and quest for applications of novel forms of cellulose, variously named crystallites, whiskers, nanocrystals, nanofibres and nanofibrils is creating plenty of activity. Novel techniques for their synthesis range from top-down approaches comprising chemical, physical or enzymatic procedures for their segregation from wood and agricultural leftovers to the bottom-up synthesis of cellulose nanofibrils from glucose by bacteria.

In a unique approach, these nanocelluloses possess significant cellulose properties such as hydrophilicity, broad chemical-modification capacity, and the development of versatile semi crystalline fibre morphologies with the specific features of nano scale elements owing to the large surface area of these materials. Based on their dimensions, functions, and preparation techniques, which consecutively are determined by mostly on the cellulosic source and on the treating conditions, nanocelluloses may be classified in three main categories which are nanocrystalline cellulose (NCC), microfibrillated cellulose (MFC) and bacterial nanocellulose (BNC).

NCCs are synthesis by the elimination of amorphous regions of a purified cellulose source by acid hydrolysis, frequently followed by ultrasonic treatment. It has very limited flexibility although comparable in size to MFC as it does not have amorphous segments but instead display lengthened crystalline rod like shapes. Depending on their biological source, NCC crystals might also express diverse geometries; for example, both bacterial and tunicate cellulose chains have twisted-ribbon geometry whereas algal cellulose membrane shows a rectangular structural orientation [2].

Many technologies, such as acid hydrolysis, enzymatic treatment, hydrothermal treatment, ultrasonication or combinations thereof have been extensively explored to isolate NCC from biomass [3-6]. Among these technologies, hydrothermal treatment become interested to be used because of its advantages, such as no catalyst requirement, less corrosion, high energy efficiency and so on [7]. Moreover, it is also efficient in hemicellulose and lignin removal as it is conducive to the dissolution of both materials. Pihlajaniemi

V, et al. reported that 86 % of lignin have been removed from wheat straw using combination of hydrothermal and alkali treatment [8].
Sulphuric acid is widely used in previous research on isolation of NCC [9,10,11]. But, in this study, Oxalic acid dihydrate is a naturally abundant, biodegradable, non-volatile, and thus a sustainable reagent was used to isolate NCC [12]. There are several researchers that used oxalic acid in isolation of NCC. Abraham E., et al. used oxalic acid to isolate nanocellulose from banana, jute and pineapple leaf fibres [13] while Sirviö, J. A., et al. has successfully isolate NCC from wood fibers using dihydrate oxalic acid [14].
The objective of this research is to isolate NCC from pulverized kenaf core. Hydrothermal treatment with low concentration of oxalic acid hydrolysis was used to isolate the cellulose. It is expected that this technique is viable for isolating NCC and less harmful to the environment.

2. Methodology

2.1. Materials

Pulverized kenaf core (PKC) powder was obtained from Kefi (Malaysia) Sdn. Bhd. Sodium hydroxide (NaOH) used for alkali treatment was purchased from Merck. Sodium hypochlorite (NaClO) and acetic acid used for bleaching process were purchased from R&M Chemical respectively. Oxalic acid dihydrate used for acid hydrolysis was purchased from R&M Chemical.

2.2. Alkali treatment

30g pulverized kenaf core (PKC) were treated using 4% w/v NaOH at 121ºC for 1 hour in an autoclave. The resulting PKC were strained and washed with distilled water and cloth filter until the alkali was completely removed. The PKC powders were then oven dried in an air-circulating oven.

2.3. Bleaching treatment

Alkaline treated PKC were bleached using a mixture of 27 wt% NaOH and acetic acid (27 g and 75.1 mL respectively) and a mixture of NaClO solutions with ratio 1:3. The ratio of PKC to liquor was 10:100 (g/mL). The bleaching was repeated 5 times. After bleaching, the bleached PKC were washed repeatedly with distilled water until the pH reached neutrality and subsequently dried in air circulating oven.

2.4. Acid Hydrolysis

5 g bleached PKC were treated with 50 ml 11 wt% oxalic acid in an autoclave at 120°C until it attained a pressure of 150 kPa. The pressure was released immediately. The resulting NCC suspension was dialysed using 3L distilled water for several days until neutral pH of 7. The resulting suspension was then sonicated using ultrasonicator.

2.5. Characterization of nanocrystalline cellulose

2.5.1. Particles size distribution and zeta potential

The particles size distribution and zeta-potentials values were determined using Zetasizer Nano-ZS (Malvern Instruments Ltd.) to examine NCC suspension size distribution, colloidal stability and electrophoretic mobility. The samples were measured after sonication.

2.5.2. Scanning electron microscope (SEM)

The surface morphology was studied by using SEM with magnification of x300 at 15 kV.

2.5.3. Fourier transform infrared (FTIR) spectroscopy

Four samples which are untreated PKC, alkaline-treated PKC, bleached PKC and NCC) were analysed using Perkin-Elmer Spectrum One. FTIR spectral analysis was performed within the wave number range of 600-4000 cm^{-1}.

2.5.4. X-ray diffraction (XRD)

X-ray diffraction was used to determine the crystallinity of the PKC after bleaching and hydrolysis treatments. The samples were analysed using Rigaku X-ray diffractometer with monochromatic Cu Kα radiation source (λ = 0.1539 nm) from 2θ = 2° to 50° with a step size of 0.05. To characterize the crystallinity of the different samples, the crystallinity index, CrI was determined using Segal's equation. It was calculated using the following equation [15];

$$\text{Crystallinity index (CrI\%)} = \frac{I_{200} - I_{am}}{I_{200}} \times 100 \quad (1)$$

where I_{002} is the maximum intensity of the (002) lattice diffraction peak and I_{am} is the intensity scattered by the amorphous part of the sample. The intensity distributed by the amorphous part is measured as the lowest intensity at a diffraction angle around 2θ = 18° [16].

3. Results and discussion

3.1. Particles size distribution and zeta potential

Fig. 1 shows the size distribution of the sonicated NCC suspension that indicates the suspension is polydisperse particles because there are three size distributions obtained from the acid hydrolysis. The distribution of NCC suspension consists of 35 % volume particle with size range of 10 to 100 nm, 28.2 % volume for range 101 to 1000 nm and the remaining 36.8 % for bigger than 1000 nm. The agglomeration of the NCC particle during sonication may promote the agglomeration of particles. However, zeta potential value of the NCC suspension is -31.6 ± mV. Particles with zeta potentials more positive than +30mV or more negative than -30mV are normally considered stable [17].

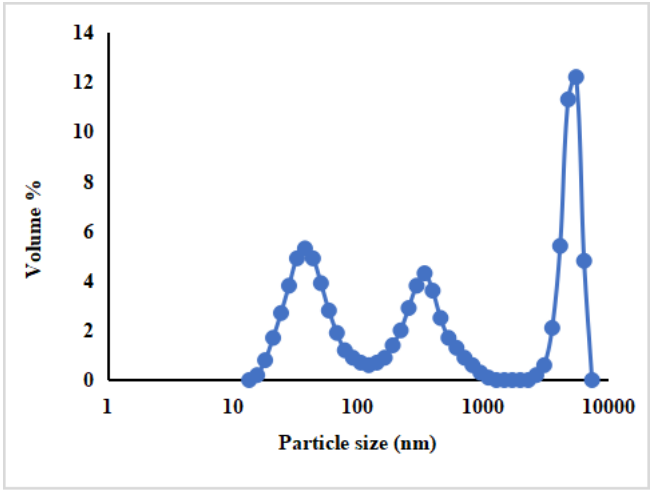

Fig. 1: Size distribution of sonicated NCC suspension

Cumulative plot of NCC size distribution is presented in Fig. 2. d_{50} also known as median diameter is the particle size at the 50 % of the cumulative graph. From Fig. 2, the d_{50} of the NCC size distribution is 316.72 nm means the particle size of 50 % of the cellulose particle in the NCC suspension is smaller than 316.72 nm. The average diameter of the NCC particle is 182.55 nm.

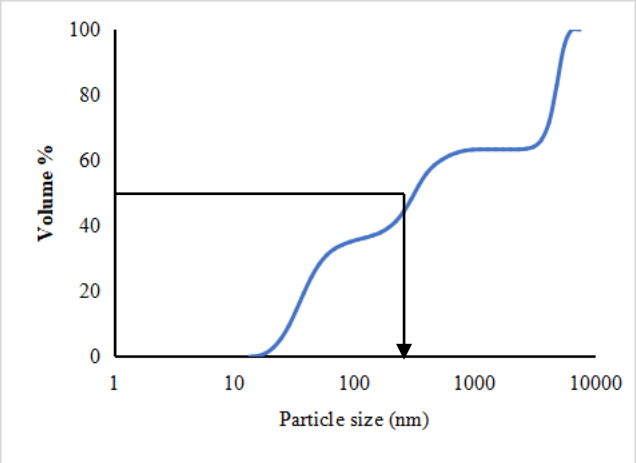

Fig. 2: Cumulative size distribution of sonicated NCC suspension

3.2. Scanning electron microscope (SEM)

Fig. 3 shows the SEM images of the dried isolated NCC from PKC. The acid hydrolysis was expected to reduce the particle size of the NCCs. The SEM image clearly shows the reduction of the NCCs size after acid hydrolysis because of the removal of amorphous structure of the bleached PKC but the sizes are not consistent. The image shows that the dried NCC particles were agglomerated as have been circled in the image. The agglomeration might due to the freeze drying process. This is a common phenomenon reported by other researchers [18].

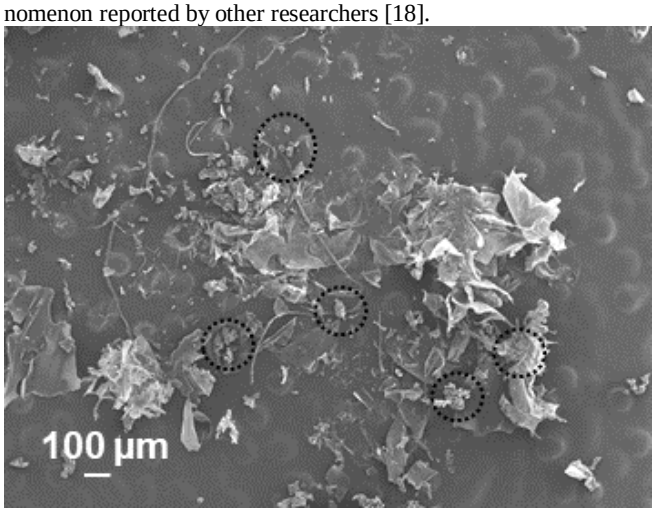

Fig. 3: SEM image of dried NCC isolated from PKC

3.3. Fourier transforms infrared (FTIR) analysis

FTIR spectroscopy was used with the purpose to reveal the composition of the PKC before and after treatments. Fig. 4 shows the FTIR spectra recorded for (a) raw PKC, (b) alkali treated PKC, (c) bleached PKC and (d) NCC suspension from PKC. The absorption peak in 3400-3300 cm^{-1}, which was observed in all spectra, is corresponded to O-H stretching and bending vibration of the cellulose's OH groups. The peak represents the intra- and intermolecular hydrogen bonds [19]. Whilst the absorption peak around 1640-1630 cm^{-1} in all spectra is due to the O-H bending and streching of hydrogen bond resulted from absorption of water [20]. These results show that the cellulose component was not removed during the chemical treatment of the PKC. The aliphatic saturated C-H stretching linked with methylene groups in cellulose was observed at around 3000-2900 cm^{-1} [21]. The peak is present in the spectra of all of the fibre components, but most remarkably in the spectra for cellulose [22,23]. The peak is the characteristic peak for NCC as it is more obvious compared to on raw, alkaline treated and bleached fibre. Absorption peak observed at around 1740 cm^{-1} in the raw kenaf fibre spectra attributed to C=O stretching of acetyl groups in hemicellulose or corresponded to the p-coumeric components of hemicellulose and/or lignin [24]. The peak disappears after alkali treatment, showing that the alkali treatment removed non-cellulosic materials [25].

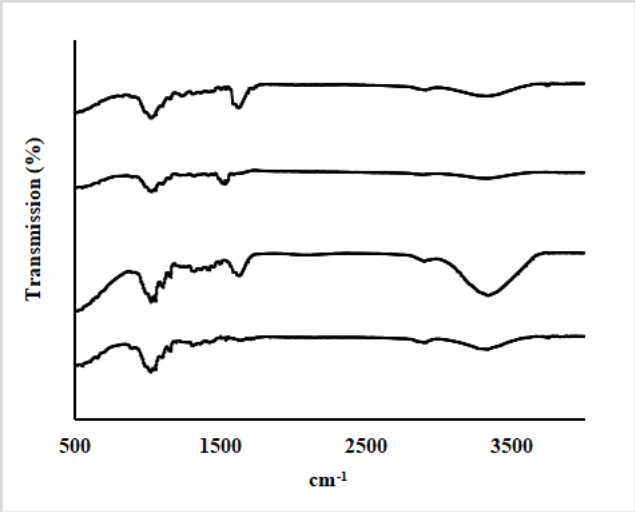

Fig. 4: FTIR spectra recorded for (a) raw PKC, (b) alkali treated PKC, (c) bleached PKC and (d) NCC suspension from PKC

The absorption peak at around 1590 cm^{-1} corresponds to the aromatic symmetric stretching in lignin [26]. However, this peak disappears after the bleaching treatment due to the removal of lignin [27]. The peak was not detected for bleached kenaf fibre and NCC. Absorption peak at around 1030 cm^{-1} is attributed to the stretching of C-O. The absorption peaks prove the existence of three polymeric constituents which are lignin, cellulose and hemicelluloses [28]. It appeared in raw PKC, alkali-treated PKC and bleached PKC. This peak is not disappearing even after the chemical treatment which indicates the presence of cellulose since the lignin and hemicellulose are removed during alkali treatment and bleaching process.

3.4. X-ray diffraction (XRD)

Cellulose has crystalline regions and amorphous regions. The unfavorable amorphous regions are crucial to be eliminated by means of chemical treatments to proficiently extract highly crystalline and purified NCC. X-ray diffraction (XRD) analysis was carried out to evaluate the crystallinity of the PKC after different chemical treatment as chemical treatment performed on PKC can affect the crystallinity of cellulose. The crystalline regions of celluloses are impenetrable by acids during the acidic incursion, but it hydrolyzed the amorphous regions to release individual crystallites [29]. The crystallinity of chemically treated PKC can be determined and compared to access the effectiveness of the chemical treatment.

Fig. 5 shows the diffraction patterns obtained for (a) after acid hydrolysis of PKC (dried NCC), (b) after bleaching of PKC. The peaks obtained from the XRD intensities were the characteristics peaks for Cellulose I [30]. These peaks become more distinct upon chemical treatment. The crystallinity index was determined for the bleached PKC and NCC, and the results are summarized in Table 1. The CrI for bleached PKC is 59.72%. Further treatment using oxalic acid increased the CrI from 59.72% for bleached PKC, to 64.29% for dried NCC sample.

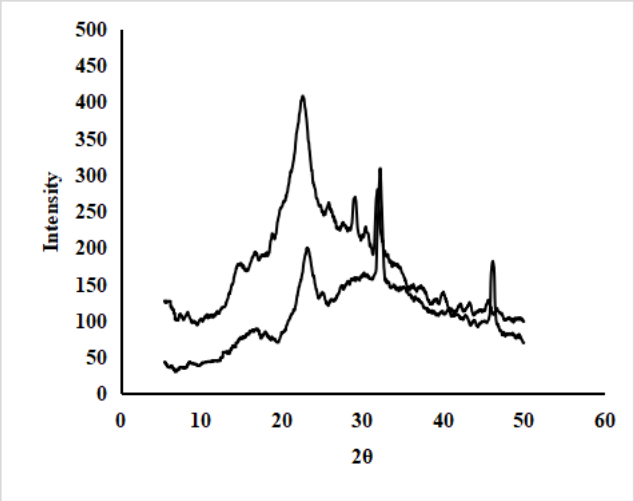

Fig. 5: XRD Intensities of (a) after acid hydrolysis of PKC (dried NCC), (b) after bleaching of PKC

The increase of the CrI value after acid hydrolysis of PKC was contributed by the elimination of amorphous regions. The core function of the acid was to disintegrate the ordered structure of the nanofibril bundles into crystalline nanocrystals by releasing hydronium ions (H+) for hydrolytic cleavage of glycosidic bonds in cellulose molecular chains inside amorphous segments alongside the cellulose fibrils [31,32]. In addition, throughout the synthesis of nanocrystalline cellulose, rearrangement of monocrystals may take place in parallel and thus increase the cellulose crystallinity [33,34].

Table 1: Cellulose intensity peak and its respective degree of crystallinity

Samples	Cellulose intensity peak (2θ)	Degree of crystallinity (%)
After acid hydrolysis of PKC (dried NCC)	22.3	64.29
After bleaching of PKC	23.15	59.72

4. Conclusion

In summary, NCCs were successfully synthesis from pulverized kenaf core via hydrothermal with low concentration of oxalic acid hydrolysis after chemical pretreatments. Zeta potential analysis shows a stable NCC suspension with value of -31.6mV. The size distribution shows polydisperse NCC particles in the suspension with median diameter, d_{50} of 316.72 nm and average diameter of 182.55 nm. The SEM image show agglomerated NCC particles after freeze drying. The purification of cellulose was performed using chemical treatments comprising of alkali and bleaching treatments. It was observed that the alkali treatment was efficient in removing hemicellulose while the bleaching treatment removed lignin. FTIR spectroscopy analysis confirmed the elimination of non-cellulosic materials. From the XRD analysis, it was shown that the oxalic acid hydrolysis induced and increased of the crystallinity index from 59.72% to 64.29%. This study suggested that hydrothermal with low concentration of oxalic acid (weak acid) can be used for isolation of NCC.

Acknowledgement

The authors would like to thank the financial support received from Research Management Institute of Universiti Teknologi MARA through Geran Inisiatif Penyeliaan (600-IRMI/GIP 5/3 (0015/2016)), Fundamental Research Grant Scheme (600-RMI/FRGS 5/3 (0095/2016)), Ministry of Higher Education, Malaysia, Faculty of Chemical Engineering, UiTM and Universiti Teknologi MARA, Malaysia.

References

[1] Abdul Khalil, H. P. S., Bhat, A. H., & Ireana Yusra, A. F. (2012). Green composites from sustainable cellulose nanofibrils: A review. Carbohydrate Polymers, 87(2), 963-979. doi:http://dx.doi.org/10.1016/j.carbpol.2011.08.078

[2] Itoh, T., & Brown Jr, R. (1988). Development of cellulose synthesizing complexes inBoergesenia andValonia. Protoplasma, 144(2-3), 160-169.

[3] Amin, K. N. M., Annamalai, P. K., Morrow, I. C., & Martin, D. (2015). Production of cellulose nanocrystals via a scalable mechanical method. RSC Advances, 5, 57133-57140.

[4] Reddy, J. P., & Rhim, J. W. (2014). Isolation and characterization of cellulose nanocrystals from garlic skin. Materials Letters, 129, 20-23.

[5] Sheltami, R. M., Abdullah, I., Ahmad, I., Dufresne, A., & Kargarzadeh, H. (2012). Extraction of cellulose nanocrystals from mengkuang leaves (Pandanus tectorius). Carbohydrate Polymers, 88, 772-779.

[6] Silvério, H. A., Neto, W. P. F., Dantas, N. O., & Pasquini, D. (2013). Extraction and characterization of cellulose nanocrystals from corncob for application as reinforcing agent in nanocomposites. Industrial Crops and Products, 44, 427-436.

[7] Wang, Z. W., Zhu, M. Q., Li, M. F., Wang, J. Q., Wei, Q., & Sun, R. C. (2016). Comprehensive evaluation of the liquid fraction during the hydrothermal treatment of rapeseed straw. Biotechnology for Biofuels, 9, 142. http://doi.org/10.1186/s13068-016-0552-8

[8] Pihlajaniemi V., Sipponen M. H., Pastinen O., Lehtomäki I. & Laakso S. (2015). Yield optimization and rational function modelling of enzymatic hydrolysis of wheat straw pretreated by NaOH-delignification, autohydrolysis and their combination. Green Chem. 17, 1683–1691.

[9] Xie, J., Hse, C. Y., De Hoop C. F., Hu T., Qi J. & Shupe T. F. (2018) Isolation and characterization of cellulose nanofibers from bamboo using microwave liquefaction combined with chemi-cal treatment and ultrasonication. Carbohydrate Polymers. 151, 725-734.

[10] Sanchez de la Concha B. B., Agama-Acevedo E., Nuñez-Santiago M. C., Bello-Perez L. A., Garcia H. S. & Alva-rez-Ramirez J. (2017) Acid hydrolysis of waxy starches with different granule size for nanocrystal production. Journal of Cereal Science. 79, 193-200.

[11] Shaheen T. I. & Emam H. E. (2018) Sono-chemical synthesis of cellulose nanocrystals from wood sawdust using Acid hy-drolysis. International Journal of Biological Macromolecules. 107, 1599-1606.

[12] Li, D., Henschen, J., & Ek, M. (2017). Esterification and hydrolysis of cellulose using oxalic acid dihydrate in a solvent-free reaction suitable for preparation of surface-functionalised cellulose nanocrystals with high yield. Green Chemistry, 19(23), 5564–5567.

[13] Abraham, E., Deepa, B., Pothan, L. A., Jacob, M., Thomas, S., Cvelbar, U., & Anandjiwala, R. (2011). Extraction of nanocellulose fibrils from lignocellulosic fibres: A novel approach. Carbohydrate Polymers, 86(4), 1468–1475.

[14] Sirviö, J. A., Visanko, M., & Liimatainen, H. (2016). Acidic Deep Eutectic Solvents As Hydrolytic Media for Cellulose Nanocrystal Production. Biomacromolecules, 17(9), 3025–3032.

[15] Segal L., Creely J., Martin Jr A. & Conrad C. (1959) An empirical method for estimating the degree of crystallinity of native cellulose using the X-ray diffractometer. Textile Research Journal. 29, 786-794.

[16] Kumar, A., Negi, Y. S., Choudhary, V., & Bhardwaj, N. K. (2014). Characterization of cellulose nanocrystals produced by acid-hydrolysis from sugarcane bagasse as agro-waste. Journal of Materials Physics and Chemistry, 2(1), 1-8.

[17] Hemraz U. D., Boluk Y. & Sunasee R. (2013) Amine-decorated nanocrystalline cellulose surfaces: synthesis, characterization, and surface properties. Canadian Journal of Chemistry. 91, 974-981.

[18] Subair N., Jinitha T. V., Shaniba V., Sreejith M.P., Aparna K. B. & Purushothaman E. (2018) Isolation and characterization of cellulose nanocrystals from sago seed shells. Carbohydrate Polymers. 180, 13-20.

[19] Khalil, H. A., Ismail, H., Rozman, H., & Ahmad, M. (2001). The effect of acetylation on interfacial shear strength between plant fibres and various matrices. European Polymer Journal, 37(5), 1037-1045.

[20] Morán, J. I., Alvarez, V. A., Cyras, V. P., & Vázquez, A. (2008). Extraction of cellulose and preparation of nanocellulose from sisal fibers. Cellulose, 15(1), 149-159.

[21] Lamaming, J., Hashim, R., Sulaiman, O., Leh, C. P., Sugimoto, T., & Nordin, N. A. (2015). Cellulose nanocrystals isolated from oil palm trunk. Carbohydrate Polymers, 127, 202-208.
[22] Poletto, M., Zattera, A. J., & Santana, R. (2012). Structural differences between wood species: evidence from chemical composition, FTIR spectroscopy, and thermogravimetric analysis. Journal of applied polymer science, 126(S1).
[23] Popescu, C.-M., Singurel, G., Popescu, M.-C., Vasile, C., Argyropoulos, D. S., & Willför, S. (2009). Vibrational spectroscopy and X-ray diffraction methods to establish the differences between hardwood and softwood. Carbohydrate Polymers, 77(4), 851-857.
[24] Joonobi, M., Harun, J., Tahir, P. M., Zaini, L. H., SaifulAzry, S., & Makinejad, M. D. (2010). Characteristic of nanofibers extracted from kenaf core. BioResources, 5(4), 2556-2566.
[25] Ouajai, S., & Shanks, R. (2005). Composition, structure and thermal degradation of hemp cellulose after chemical treatments. Polymer Degradation and Stability, 89(2), 327-335.
[26] Kumar, A., Negi, Y. S., Bhardwaj, N. K., & Choudhary, V. (2012). Synthesis and characterization of methylcellulose/PVA based porous composite. Carbohydrate Polymers, 88(4), 1364-1372.
[27] Yan, T., Xu, Y., & Yu, C. (2009). The isolation and characterization of lignin of kenaf fiber. Journal of applied polymer science, 114(3), 1896-1901.
[28] Islam M. S., Hasbullah N. A. B., Hasan M., Talib Z. A., Jawaid M. & Haafiz M. M. (2015) Physical, mechanical and biodegradable properties of kenaf/coir hybrid fiber reinforced polymer nanocomposites. Materials Today Communications. 4, 69-76.
[29] Peng, B. L., Dhar, N., Liu, H., & Tam, K. (2011). Chemistry and applications of nanocrystalline cellulose and its derivatives: a nanotechnology perspective. The Canadian Journal of Chemical Engineering, 89(5), 1191-1206.
[30] Chan H. C., Chia C. H., Zakaria S., Ahmad I. & Dufresne A. (2012) Production and characterisation of cellulose and nano-crystalline cellulose from kenaf core wood. BioResources. 8, 785-794.
[31] de Souza Lima M. M. & Borsali R. (2004) Rodlike cellulose microcrystals: structure, properties, and applications. Macromolecular Rapid Communications. 25, 771-787.
[32] Tee T. T., Sin L. T., Gobinath R., Bee S. T., Hui D. & Rahmat A. R. (2013) Investigation of nano-size montmorillonite on enhancing polyvinyl alcohol–starch blends prepared via solution cast approach. Composites Part B: Engineering. 47, 238-247.
[33] Li, Q., Zhou, J., & Zhang, L. (2009). Structure and properties of the nanocomposite films of chitosan reinforced with cellulose whiskers. Journal of Polymer Science Part B: Polymer Physics, 47(11), 1069-1077.
[34] Li, R., Fei, J., Cai, Y., Li, Y., Feng, J., & Yao, J. (2009). Cellulose whiskers extracted from mulberry: A novel biomass production. Carbohydrate Polymers, 76(1), 94-99.